
Article:
Cross, Mathew J, Sajjad, M Arif, Macgregor, Stuart A et al. (1 more author) (2025) Square Planar Ru(iPr2PCH2CH2NH)2 and its Role in Fast and Selective Catalytic Amine-Borane Dehydropolymerization to Form High Molecular Weight Polyaminoboranes. Angewandte Chemie International Edition. e202500019. ISSN 1433-7851

https://doi.org/10.1002/anie.202500019

Square Planar Ru(^{i}Pr$_2$PCH$_2$CH$_2$NH)$_2$ and its Role in Fast and Selective Catalytic Amine-Borane Dehydropolymerization to Form High Molecular Weight Polyaminoboranes.

Mathew J. Cross,[a] M. Arif Sajjad,[b] Stuart A. Macgregor,[b]* Andrew S. Weller [a]*

[a] Mr M. J. Cross, Prof. A. S. Weller
Department of Chemistry, University of York,
Heslington, York, YO10 5DD, UK
Email: andrew.weller@york.ac.uk

[b] Dr M. A. Sajjad, Prof. S. A. Macgregor
EaStCHEM School of Chemistry, University of St Andrews
North Haugh, St Andrews, KY16 9ST, UK
Email: sam38@st-andrews.ac.uk

Dedicated to the memory of Ian Manners. A pioneer in the field of amine-borane dehydropolymerization, mentor and friend.

Abstract: Addition of ^{t}BuOK to orange RuCl$_2$(^{i}Pr$_2$PCH$_2$CH$_2$NH$_2$)$_2$ forms the pink, square planar, Ru(II) complex Ru(^{i}Pr$_2$PCH$_2$CH$_2$NH)$_2$. This is an active catalyst (ToF 250 s^{-1}) for the dehydropolymerization of H$_3$B·NMeH$_2$ to give high molecular weight polyaminoborane, [H$_2$BNMeH]$_n$ (M_n = 138,700 g mol^{-1}) at low loadings (0.03 mol%). An induction period observed is due to the initial formation of a hydroxy-hydride species Ru(^{i}Pr$_2$PCH$_2$CH$_2$NH$_2$)$_2$(OH)(H), prior to fast turnover.

Polyaminoboranes (PABs), such as –[H$_2$BNMeH]$_n$– Me-PAB, are polymers which have main-chain B–N backbones, and are isoelectronic with polyolefins.[1-3] As well as the fundamental interest associated with the selective and controlled synthesis of main-group polymers,[4, 5] PABs are also polymeric precursors to BN-based ceramics.[6]

The catalytic dehydropolymerization of commercially available H$_3$B·NMeH$_2$ is a potentially efficient and controllable method to manufacture Me-PAB.[7, 8] This is a cascade polymerization,[9] Fig. 1A, that sequentially couples an initial catalytic dehydrogenation of H$_3$B·NMeH$_2$ to form a reactive amino-borane, monomer H$_2$B=NMeH,[10] with a subsequent, fast, nucleophilic head-to-tail, non-living, chain-growth propagation promoted by an initiator (likely a metal hydride[11] or amine[12]). Exemplar pre-catalyst systems are shown in Fig. 1B.[1, 2, 13-15] Stoichiometric methods that do not use transition metal catalysts,[12] or where catalytic step-growth polymerization is invoked, have also been reported.[16] While the initiation and termination events are still not well understood, molecular weight can be controllably reduced by use of a chain-control additive,[17] and for some systems variation in catalyst loading results in higher degrees of polymerization.[14, 16] Systems that operate at low loadings to selectivity produce high molecular weight Me-PAB (i.e.,>100,000 g mol^{-1}[18]) would be particularity useful, as increasing molecular weight allows for the tuning of the materials properties of Me-PAB for subsequent processing, e.g. the production of BN ceramics with low residual metal content.[19]

The Me-PAB chain growth mechanism is related to classical anionic and radical polymerizations,[20] for which the degree of polymerization (D.P.) depends on the rate of propagation/rate of termination, i.e. D.P. $\propto R_{(prop)}/R_{(term)}$. This suggests that a fast H$_3$B·NMeH$_2$ dehydrogenation catalyst would result in high degrees of polymerization, assuming any termination events are catalyst-independent. Such a system was reported by Fagnou in 2008,[21] using the metal/ligand cooperative[22-24] pre-catalyst *P,P-cis*-RuCl$_2$(^{i}Pr$_2$PCH$_2$CH$_2$NH$_2$)$_2$ **1** (0.5 mol%). When activated with 30 equivalents of ^{t}BuOK, dehydrogenation is very rapid, but was unselective for Me-PAB.[25] A refinement by Manners, using low temperatures, produces Me-PAB, but isolated polymer was of low-molecular weight (M_n = 26,000 g mol^{-1}, $Đ$ = 3.4).[2] As strong nucleophiles/bases can promote the depolymerization of Me-PAB,[13, 26, 27] the large excess of ^{t}BuOK used likely impacts selectivity, while the identity of the active catalyst has not been determined.

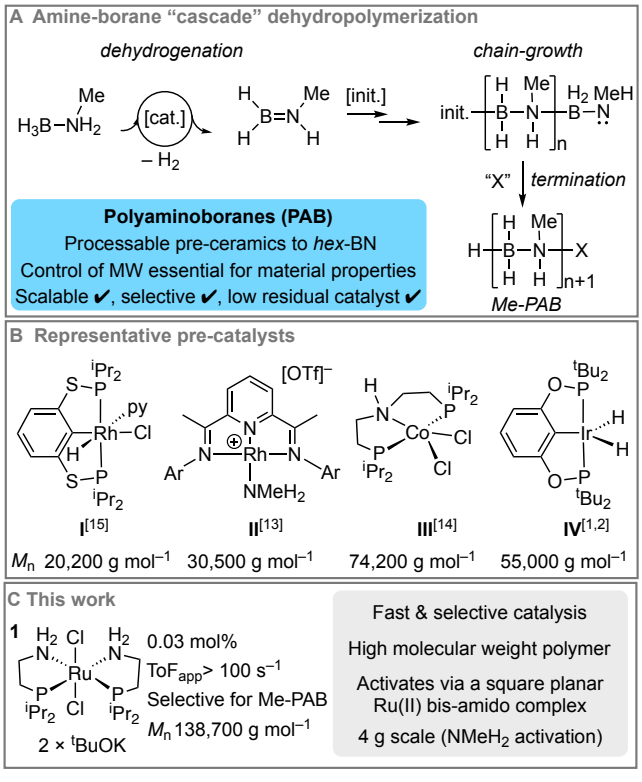

Figure 1 A) Cascade amine-borane dehydropolymerization. **B)** Representative comparisons of selected catalysts. **C)** This work: fast and selective dehydropolymerization to give high molecular weight Me-PAB.

We now describe that precise activation of **1** with two equivalents of ^{t}BuOK promotes the formation of high molecular weight Me-PAB. Catalysis is exceptionally fast (ToF ~250 s^{-1}), and selective (>99%). We show that the first formed species is a square planar Ru(II) complex.[28, 29] This reacts with adventitious water present in the system to form a hydroxy-hydride, that also is a competent pre-catalyst. We also report that **1** can be expediently activated with $NMeH_2$, to produce high molecular weight Me-PAB on a 4 g scale, and that the catalyst formed under these conditions is likely the same as with ^{t}BuOK.

Addition of 2 equivalents of ^{t}BuOK to a THF solution of orange **1**[30] resulted in a change in color over 30 minutes to give a highly air-sensitive deep pink solution, Fig. 2A. A portion of this solution was added to recrystallized $H_3B{\cdot}NMeH_2$ (1 M in THF, 112 mg) at 20 ºC to give a $[Ru]_{TOTAL}$ of 0.03 mol%. Subsequent dehydropolymerization reaction progress was measured by H_2 evolution using a water-filled eudiometer. After a long (and rather stochastic, multiple repeats) induction period of ~1500s rapid catalysis occurs [*caution, H_2 release*] so that one equivalent of H_2 evolved in ~270 s (TON ≈ 3300). The initial kinetics of productive turnover showed a pseudo-zero order region (TOF_{app}[31] of ~100 s^{-1}), followed by a deceleration in rate, Fig. 2B. This is one of the fastest dehydropolymerization catalyst systems reported.[24] Precipitation of the solution in pentane recovered $[H_2BNMeH]_n$ in 60% isolated yield and >99% selectivity, as shown by ^{11}B NMR spectroscopy, Fig. 2C.[2] Analysis by GPC (Gel Permeation Chromatography, relative to polystyrene standards[8]) demonstrated a mono-modal distribution of high-molecular weight polymer M_n = 138,700 g mol^{-1}, $Đ$ = 1.48 (Fig. S13). Use of 30 equivs of ^{t}BuOK resulted in the unselective formation of BN-products, including *N,N,N*-trimethyl borazine, and greater than 2 equivalents of H_2 are released, as reported by Fagnou.[21]

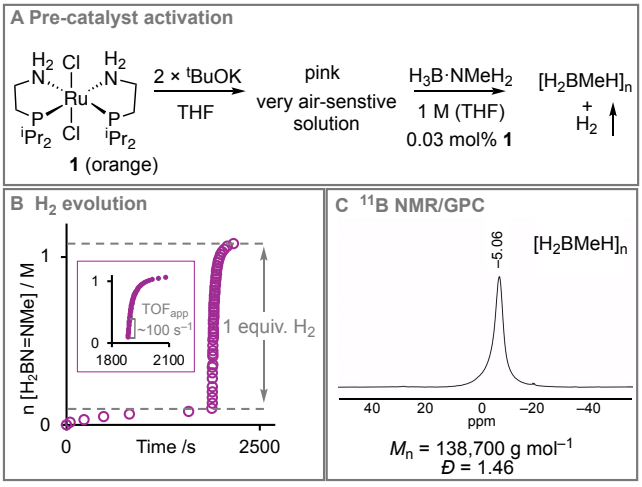

Figure 2 A) Pre-catalyst activation. **B)** Representative reaction progress plot [H_2B=NMeH] equivalents from H_2 evolution (0.03 mol %, **1**). Inset shows the region of fast turnover. **C)** In situ ^{11}B NMR spectrum of the catalysis mixture (THF) and GPC data for the isolated polymer.

This remarkably fast catalysis prompted the investigation of the initially formed pink species. It is well-established that ^{t}BuOK acts to dehydrohalogenate Ru-amine precursors,[22, 32] and Fagnou proposed 16 electron $RuH(^{i}Pr_2PCH_2CH_2NH)(P^{i}Pr_2CH_2CH_2NH_2)$, **A**, as the active species in amine-borane dehydrogenation.[21] Addition of 2 equivalents of ^{t}BuOK to **1** in THF resulted in a pentane-soluble deep-pink complex, that was isolated as highly air-sensitive crystalline material in low (18%) yield from recrystallization at –80 ºC. Analysis by single-crystal X-ray diffraction and NMR spectroscopy showed these crystals to be the formally 14-electron Ru(II) complex *P,P-trans*-$Ru(^{i}Pr_2PCH_2CH_2NH)_2$, **2**. The low isolated yield is accounted for by **2**'s solubility in pentane, as in situ NMR spectroscopy shows the formation of **2** from **1** to be quantitative. The solid-state molecular structure of complex **2** as determined by single-crystal X-ray diffraction is shown in Figure 3.

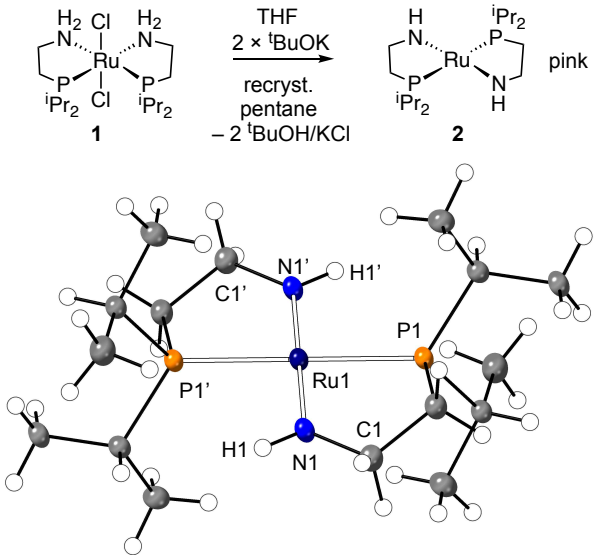

Figure 3 Synthesis and molecular structure of complex **2**. Displacement ellipsoids are shown at the 50% probability level. H1/H1' were located. Selected bond lengths [Å] and angles [°]: Ru1–N1 1.931(2), Ru1– P1 2.2943(6), C1–N1 1.473(3); P1–N1–Ru1 82.45(7), P1–Ru1–N1 97.55(7), N1–Ru1–N1 180.0, P1–Ru1–P1' 180.00(3).

Complex **2** has a, d^6, square-planar Ru(II) center coordinated with two chelating ligands, with the phosphines now *trans* orientated. The Ru atom sits on an inversion center, and the RuN2P2 atoms lie in a crystallographically-imposed plane. The proton on N1 (H1) was located, and the sum of angles around N1 = 360º. The C1–N1 distance [1.473(3) Å] is consistent with a single bond. These data signal a sp^2 amido group. Compared with the *trans*-isomer of **1** (see Supporting Materials) the Ru–N distance in **2** is shorter, 1.931(2) Å versus 2.142(4) Å, suggesting a degree of N–Ru pπ–dπ bonding. Similar, short, Ru–N bond lengths have been noted in the other, albeit rare, examples of square planar Ru(II) complexes that all contain amido-ligands.[28, 29, 33, 34] The solution NMR data (C_6D_{12}, 298 K) acquired immediately after dissolution of the crystals show a diamagnetic complex with high symmetry, consistent with the solid-state structure. Notably the amido protons are observed at δ 5.95 as a single, relative integral 2H, peak,[32] and only two sets of signals are observed for the diastereotopic ^{i}Pr-methyl groups. No hydride signals are observed. In the $^{31}P\{^{1}H\}$ NMR spectrum a single environment is observed at δ 74.4. In the UV-vis spectrum two intense ligand to metal charge transfer bands are observed at 310 and 357 nm, with a weaker d-

d band at 522 nm. These assignments were supported by TD-DFT calculations (Fig. S60-63) and a computational study of the electronic structure of **2**. Optimization in C_i symmetry (BP86 functional) provided good agreement with the M-ligand distances (Ru–N1$_{calc}$ = 1.94 Å; Ru–P1$_{calc}$ = 2.32 Å) and confirmed the planar geometry around the N atoms. An alternative triplet state was 16 kcal/mol higher in energy. The computed singlet electronic structure is consistent with a d^6 electron count with occupied d_{x2-y2}, d_{yz} and d_{z2} orbitals (43a_g-45a_g, Figure 4). The LUMO of the system is an antibonding combination of the d_{xz} orbital with the out-of-phase combination of N p_z orbitals;[32] the corresponding bonding combination (42a_g, –5.82 eV) provides N(2p)→Ru(dπ) π-stabilization of an otherwise formally 14 electron Ru(II) center.

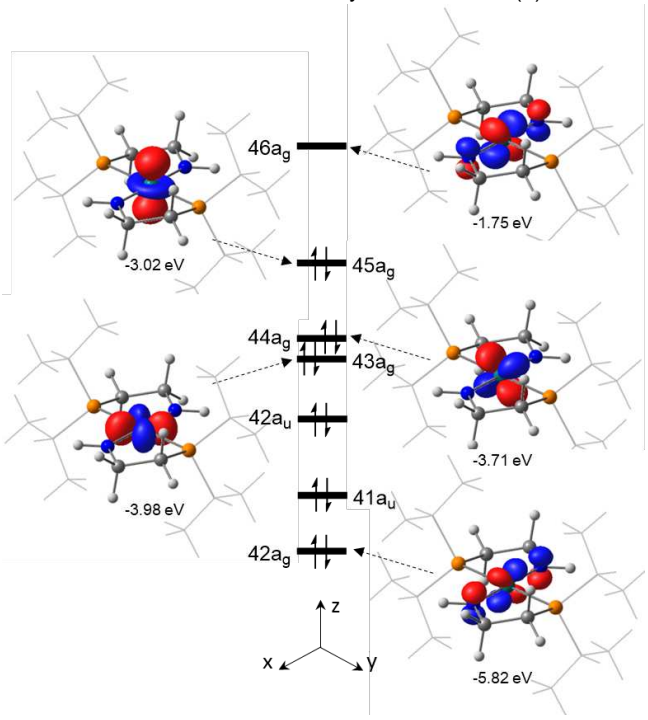

Figure 4 Kohn-Sham frontier molecular orbitals (BP86) computed for **2** (contour value = 0.107) with orbitals energies indicated. Central atoms depicted in ball and stick mode and ^{i}Pr groups in wireframe.

Complex **2** decomposes rapidly in CD_2Cl_2, but is more stable in d^8-THF or C_6D_{12}. The reactive nature of complex **2** is further revealed in its spontaneous, but relatively slow, dimerization in solution at room temperature (24 h to 1 week, depending on relative concentration) to form $Ru_2H(\mu_2\text{-}NHCH_2CH_2P^iPr_2)_2(\mu_2\text{-}NCH_2CH_2P^iPr_2)(^iPr_2PCH_2CH_2NH_2)$, **3**, which is isolated as pale-yellow crystals from a cold (–80 ºC) pentane solution. The molecular structure of complex **3** as determined by single-crystal X-ray diffraction is shown in Figure 5, which is fully supported by NMR and ESI-MS data. Dimerization results from the formation of bridging amido (N2, N3) and imino (N1) groups, the latter associated with the transfer of two hydrogens to form an amine (N4) and a Ru–hydride.[29] The hydrogen atoms associated with the N-atoms were located. Each Ru-center is six-coordinate, formally Ru(II)/18 electron. In the ^{1}H NMR spectrum multiple overlapping signals in the aliphatic/NH region are observed, but clear integral 1H multiplets at δ 8.05 and δ –11.52, that both collapse on decoupling ^{31}P, are assigned to imine (C32) proton and Ru–H, respectively. In the ^{31}P{^{1}H} NMR spectrum four sets of mutually coupled signals are observed between 77 and 60 ppm.

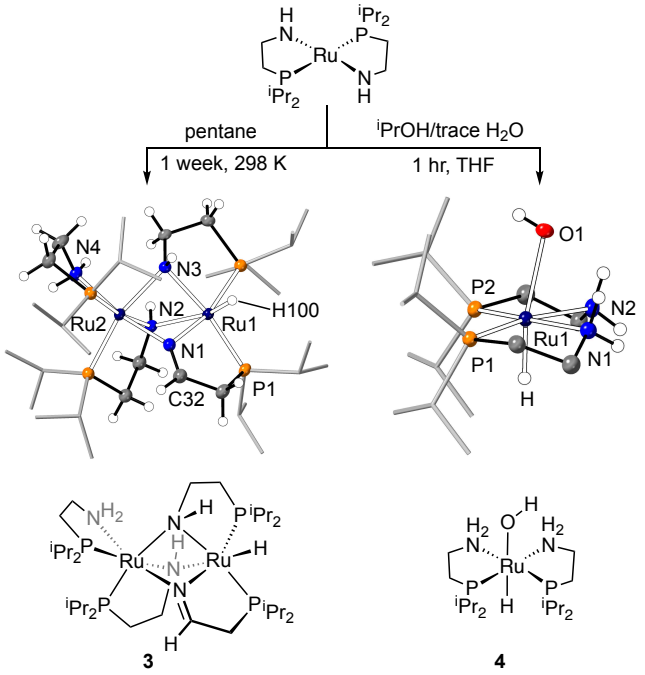

Figure 5 Synthesis and molecular structures of complexes **3** and **4**·(^{i}PrOH)$_2$. Displacement ellipsoids are shown at the 50% probability level. Only located and refined hydrogen atoms shown. ^{i}Pr groups are shown in stick form. HO^{i}Pr are not shown (see Fig. S8). Selected bond lengths [Å] and angles [°]: **3**: Ru1–N1, 2.059(2); Ru1–N2, 2.302(2); Ru1–N3, 2.159(2); Ru2–N1, 2.036(2); Ru2–N2, 2.159(2); Ru2–N3, 2.178(2); Ru2–N4, 2.178(2); N1–C32, 1.263(4); **4:** Ru1–N1, 2.186(2); Ru1–N2, 2.186(2); Ru–O1, 2.2795(18); O1–Ru1–H, 169.1(15).

The metal/ligand cooperative dehydrogenation of ^{i}PrOH by H_2 addition across Ru-amido groups is a common step in transfer hydrogenation reactions.[22, 35] Addition of five equivalents of ^{i}PrOH to *in situ* formed **2** (in THF) resulted in an immediate color change from pink to yellow. ^{31}P{^{1}H} NMR spectroscopy showed the quantitative formation of a new species by a single peak observed at δ 89.2. This new species readily decomposed on application of a vacuum, and so the solvent was removed by an argon flow prior to recrystallization from cold (–80 ºC) pentane. Multiple crops of yellow single crystals were obtained, which single-crystal X-ray diffraction showed to be the hydroxy-hydride species *P,P-cis*-Ru(^{i}Pr$_2$PCH$_2$CH$_2$NH$_2$)$_2$(OH)(H)·(^{i}PrOH)$_n$ (n = 0 and 2), **4**. Figure 5 shows the structure of **4**·(^{i}PrOH)$_2$. The ^{i}PrOH are not shown but form a bifurcated H-bonded motif with the hydroxyl group, see Fig. S8. The Ru–OH and Ru–H groups were both located and refined, and sit *trans* to one another. The, now protonated, aminophosphine ligand adopts a *cis*-P,P coordination geometry, as found for **1**. The Ru–N distances are lengthened from **2** [2.186(2) Å], and the Ru–O distance [2.2795(18) Å] sits at the upper end of the range for other reported examples of *trans*-Ru-hydroxy-hydrides [2.190(2) – 2.261(2) Å],[36-38] a distance no-doubt also influenced by the differing degree of H-bonding observed in all these complexes. In the room temperature ^{1}H NMR spectrum of **4**·(^{i}PrOH)$_n$, the Ru–H group is observed as a broad signal at ~δ –21.7. Based on ^{1}H/^{1}H COSY and ^{1}H/^{13}C

HMBC experiments the NH and OH signals are tentatively assigned to signals at ~δ 4.20 and ~3.80 respectively. These signals move slightly with differing degrees of ^{i}PrOH solvation, consistent with different degrees of hydrogen bonding/exchange.[36, 37] The IR spectrum shows weak stretches at ~3200 and 1986 cm^{-1} assigned to the Ru–OH and Ru–H, respectively.[37]

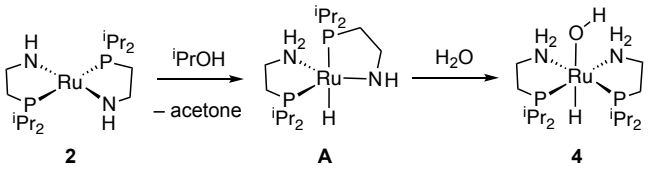

Scheme 1 Proposed mechanism for the formation of **4**

As outlined by Morris for related systems,[36] complex **4** likely results from initial transfer hydrogenation of **2** with ^{i}PrOH to form a reactive amino-hydride complex, **A** and acetone (observed), Scheme 1. Distorted trigonal bipyramidal,[32, 39] 16-electron, **A** then reacts rapidly with adventitious water present to form **4**. Off-cycle hydroxide and dimeric decomposition products have been proposed in Noyori-type amido-/amine-catalyst systems.[40]

With the identity, and reactivity, of complex **2** in hand, the mechanistic details of the induction period and productive catalytic turnover were investigated ([Ru] = 0.03 mol%). During the induction period ^{31}P{^{1}H} and ^{1}H NMR spectroscopy (–90 ºC, 512 scans) showed that hydroxy-hydride **4** was formed as the principal species (detection limit ~5%, Figs. S39). Once catalysis started this changed to a new species that showed very weak signals at ~δ –12 and δ 84 in the ^{1}H and ^{31}P{^{1}H} NMR spectra respectively, the former potentially signaling a hydride *trans* to a strong sigma-donor, possibly another hydride.[32, 41, 42] No dimer, **3**, was observed. We propose that during the induction period trace water (~0.55 mM in THF, ~10 ppm from Karl Fischer titration) is selectivity, and relatively slowly, processed by the catalyst system and $H_3B{\cdot}NMeH_2$, to ultimately form borates.[43, 44] Complex **4** thus acts as a reporter for the presence of trace water during the induction period. Once excess water is consumed rapid, and productive, catalysis starts, Fig. 6A. Support for this hypothesis comes from a number of observations. Reducing the water content using THF that had been stored over a potassium mirror resulted in no induction period (Fig. S55).[45] Adding 500 equivalents of water results in a very long induction period of ~5 hours, and at the end of catalysis a significant amount of a new species at ~δ 2ppm is observed, that is assigned to $[B(OH)_4]^-$ (Fig. S52).[44] Finally, *in situ* generated complex **4** is an active pre-catalyst for dehydropolymerization (M_n = 132,600 g mol^{-1}, $Đ$ = 1.45) after a significant induction period (Fig. S42).

Variation of [**2**] (0.016 mol% – 0.05 mol%, 1 M $H_3B{\cdot}NMeH_2$, 20 ºC) and measurement of $k_{(obs)}$ from the pseudo zero order region of H_2 evolution, immediately after induction, resulted in a non-zero intercept for $[Ru]_{TOTAL}$ (Fig. 6B). This is interpreted as decomposition of the pre-catalyst by a trace impurity that is consistently present in all catalyst runs – likely O_2 that forms paramagnetic Ru(III) complexes.[46] Titration by variation of $[Ru]_{TOTAL}$ showed this to be equivalent to 0.16 mM. An adjusted $k_{(obs)}/[Ru]_{active}$ plot is now a straight line that passes through the origin: i.e., first order in [Ru]. The role of trace impurities in modifying $[cat]_{TOTAL}$ has been noted previously.[17, 47] Using the refined catalyst loadings the TOF is now ~250 s^{-1}. For all but the lowest loadings, the degree of polymerization is relatively constant, Me-PAB M_n 117,200–141,600 g mol^{-1}, while the induction period gets shorter with higher $[Ru]_{active}$ – consistent with the processing of trace impurity (water) by **4** (Fig. S53).[48] Given the potential complicating role trace modifiers have on kinetics, the variation of $[H_3B{\cdot}NMeH_2]$ or H/D isotope effects have not been studied. The solution post-catalysis is clear, transparent and not noticeably darkened, while addition of sub-stoichiometric PMe_3 (0.5 equiv., $[Ru]_{TOTAL}$ = 0.03 mol% **2**) significantly slowed, but did not halt, catalysis compared with when no PMe_3 is added ($k_{(obs)}$ = 0.023(2) mol s^{-1}, versus 0.034(2) mol s^{-1} respectively). These observations suggest a homogenous system operates.[49]

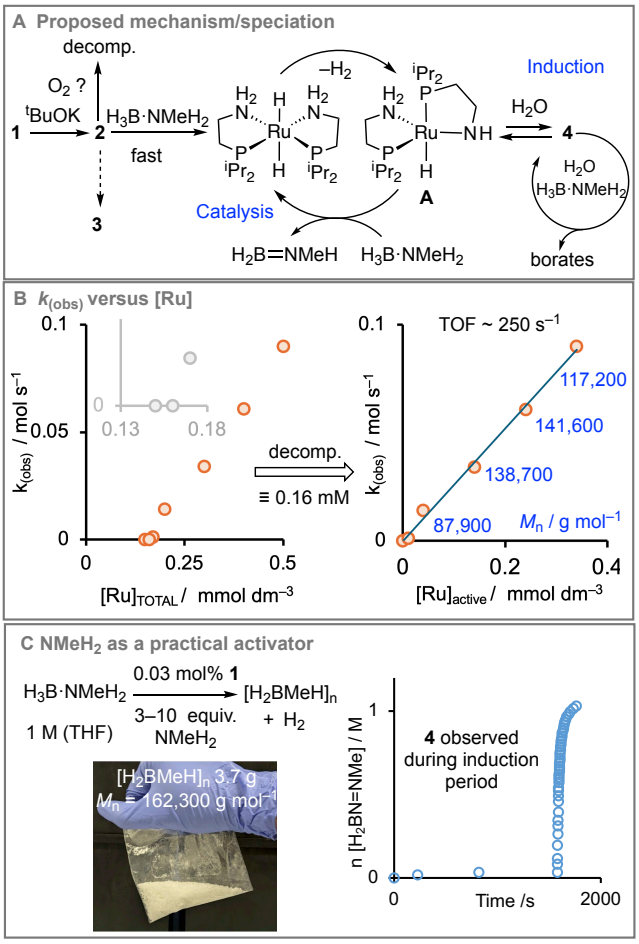

Figure 6 A) Proposed – telescoped – catalytic manifold.. **B)** $k_{(obs)}$ versus [Ru] showing the adjustment for an equivalent of a 0.16 mM impurity. Insert shows the region around $[Ru]_{TOTAL}$ = 0.16 mM. Numbers in blue are data from GPC analysis of the isolated polymer ($Đ$ ~1.5) **C)** Synthesis of Me-PAB on ~4 g scale, representative time/reaction progress plot (THF, 20 ºC).

With such efficient, and repeatable, catalysis starting from the highly air-sensitive amido-complex **2**, the use of other more practical ways of activating the starting complex **1** were explored. Amines are well-known to activate Ru–Cl complexes to form hydrides,[50] and we have shown that added amine can act as a promoter for Rh-catalyzed $H_3B{\cdot}NMeH_2$ dehydropolymerization.[13,

[14, 51] While complex **1** is not active in catalysis (monitoring for ~4 hours), addition of $NMeH_2$ (3 equiv., 0.03 mol% **1**) resulted in productive and fast turnover after a ~1500 s induction period, during which time hydroxy-hydride, complex **4,** is identified as the main species present. High molecular weight Me-PAB is formed M_n = 108,200 g mol^{-1}, $Đ$ = 1.41). This expedient method also allows for the reliable formation of high-molecular weight Me-PAB as a white powder on a ~4 g scale (10 equiv. $NMeH_2$, 0.03 mol% **1**, M_n = 162,300 g mol^{-1}, $Đ$ = 1.54, Fig. 6C).

By use of precisely 2 equivalents of activating ^{t}BuOK, the simple $RuCl_2(^iPr_2PCH_2CH_2NH_2)_2$ pre-catalyst is a remarkably selective and fast system for $H_3B{\cdot}NMeH_2$ dehydropolymerization, to form high molecular weight *N*-methyl polyaminoborane. This very fast dehydrogenation leading to high degrees of polymerization provides a simple strategy for polymer control. Identification of the first formed species as a Ru(II) square planar bis-amido complex, its evolution to a hydroxy hydride during an induction period, and the resulting kinetics of turnover, provide insight into how trace amounts of water, or other impurities, can have a profound influence on the evolution of a catalyst system operating at very low catalyst loadings. Understanding how to mitigate for, or even productively harness, such persistent trace impurities is thus important in amine-borane dehydropolymerization, something that has long been recognized in olefin-polymerization.[52]

Supporting Information

The data that support the findings of this study are available in the supplementary material of this article. Depositions 2386380 (*trans*-**1**), 2386379 (**2**), 2386381 (**3**), 2386387 (**4**·(^{i}PrOH)$_2$), 2386384 (**4**) contain the supplementary crystallographic data for this paper. These data are provided free of charge by the joint Cambridge Crystallographic Data Centre and Fachinformationszentrum Karlsruhe "http://www.ccdc.cam.ac.uk/structures".

Acknowledgements

Ms C. van Beek, Dr J. Goodall, Dr K. Altus, Profs. A. Buchard, D. Haddleton, and R. Perutz for insightful comments. The University of York (MJC), EPSRC (EP/W015498/2, SAM) for funding. We thank the referees for their perspicacious comments.

Keywords: amine-borane dehydropolymerization – catalysis – cooperative ligands – mechanism – DFT

REFERENCES

[1] A. Staubitz, A. Presa Soto, I. Manners, *Angew. Chem. Int. Ed.* **2008**, *47*, 6212-6215.

[2] A. Staubitz, M. E. Sloan, A. P. M. Robertson, A. Friedrich, S. Schneider, P. J. Gates, J. Schmedt auf der Günne, I. Manners, *J. Am. Chem. Soc.* **2010**, *132*, 13332-13345.

[3] A. Staubitz, J. Hoffmann, P. Gliese, in *Smart Inorganic Polymers* (Eds.: E. Hey-Hawkins, M. Hissler), Wiley-VCH, Weinheim, **2019**, pp. 17-39.

[4] F. Vidal, F. Jäkle, *Angew. Chem. Int. Ed.* **2019**, *58*, 5846-5870.

[5] A. M. Priegert, B. W. Rawe, S. C. Serin, D. P. Gates, *Chem. Soc. Rev.* **2016**, *45*, 922-953.

[6] E. M. Leitao, T. Jurca, I. Manners, *Nature Chem.* **2013**, *5*, 817-829.

[7] D. Han, F. Anke, M. Trose, T. Beweries, *Coord. Chem. Rev.* **2019**, *380*, 260-286.

[8] A. L. Colebatch, A. S. Weller, *Chem. Eur. J.* **2019**, *25*, 1379-1390.

[9] G. I. Peterson, T.-L. Choi, *Chem. Sci.* **2020**, *11*, 4843-4854.

[10] O. J. Metters, A. M. Chapman, A. P. M. Robertson, C. H. Woodall, P. J. Gates, D. F. Wass, I. Manners, *Chem. Commun.* **2014**, *50*, 12146-12149.

[11] S. Bhunya, T. Malakar, A. Paul, *Chem. Commun.* **2014**, *50*, 5919-5922.

[12] M. Devillard, C. A. De Albuquerque Pinheiro, E. Caytan, C. Roiland, C. Dinoi, I. Del Rosal, G. Alcaraz, *Adv. Syn. Catal.* **2021**, *363*, 2417-2426.

[13] M. J. Cross, C. N. Brodie, D. G. Crivoi, J. C. Goodall, D. E. Ryan, A. J. Martínez-Martínez, A. Johnson, A. S. Weller, *Chem. Eur. J.* **2023**, *29*, e202302110.

[14] T. M. Boyd, K. A. Andrea, K. Baston, A. Johnson, D. E. Ryan, A. S. Weller, *Chem. Commun.* **2020**, *56*, 482-485.

[15] P. Hasche, J. Haak, F. Anke, C. Kubis, W. Baumann, H.-J. Drexler, H. Jiao, T. Beweries, *Catalysis Science & Technology* **2021**, *11*, 3514-3526.

[16] T. Jurca, T. Dellermann, N. E. Stubbs, D. A. Resendiz-Lara, G. R. Whittell, I. Manners, *Chem. Sci.* **2018**, *9*, 3360-3366.

[17] C. N. Brodie, T. M. Boyd, L. Sotorríos, D. E. Ryan, E. Magee, S. Huband, J. S. Town, G. C. Lloyd-Jones, D. M. Haddleton, S. A. Macgregor, A. S. Weller, *J. Am. Chem. Soc.* **2021**, *143*, 21010-21023.

[18] D. A. Resendiz-Lara, G. R. Whittell, E. M. Leitao, I. Manners, *Macromolecules* **2019**, *52*, 7052-7064.

[19] D. Gonzalez-Ortiz, C. Salameh, M. Bechelany, P. Miele, *Mat. Today Adv.* **2020**, *8*, 100107.

[20] G. Odian, *Principles of Polymerization*, 4th ed., Wiley, Hoboken, **2004**.

[21] N. Blaquiere, S. Diallo-Garcia, S. I. Gorelsky, D. A. Black, K. Fagnou, *J. Am. Chem. Soc.* **2008**, *130*, 14034-14035.

[22] S. E. Clapham, A. Hadzovic, R. H. Morris, *Coord. Chem. Rev.* **2004**, *248*, 2201-2237.

[23] T. Higashi, S. Kusumoto, K. Nozaki, *Chem. Rev.* **2019**, *119*, 10393-10402.

[24] A. N. Marziale, A. Friedrich, I. Klopsch, M. Drees, V. R. Celinski, J. Schmedt auf der Günne, S. Schneider, *J. Am. Chem. Soc.* **2013**, *135*, 13342-13355.

[25] This reported reaction is characterized by a very fast initial H_2 loss (10 s) to form Me-PAB (NMR) but no GPC data was provided. The second loss of H_2 forms a mixture of products.

[26] N. L. Oldroyd, S. S. Chitnis, E. A. LaPierre, V. T. Annibale, H. T. G. Walsgrove, D. P. Gates, I. Manners, *J. Am. Chem. Soc.* **2022**, *144*, 23179-23190.

[27] N. E. Stubbs, T. Jurca, E. M. Leitao, C. H. Woodall, I. Manners, *Chem. Commun.* **2013**, *49*, 9098-9100.

[28] L. A. Watson, O. V. Ozerov, M. Pink, K. G. Caulton, *J. Am. Chem. Soc.* **2003**, *125*, 8426-8427.

[29] B. Askevold, M. M. Khusniyarov, E. Herdtweck, K. Meyer, S. Schneider, *Angew. Chem. Int. Ed.* **2010**, *49*, 7566-7569.

[30] W. Jia, X. Chen, R. Guo, C. Sui-Seng, D. Amoroso, A. J. Lough, K. Abdur-Rashid, *Dalton Trans.* **2009**, 8301-8307.

[31] TOF_{app} = $TOF_{apparent}$. As we show that $[cat]_{active}$ is considerably lower than $[cat]_{total}$, TOF_{app} represents the lower bound for activity. For a discussion of the use of TOF_{app} see: Crooks, A. B.; Yih, K.-H.; Li, L.; Yang, J. C.; Özkar, S.; Finke, R. *ACS Catal.* **2015**, *5*, 3342−3353.

[32] K. Abdur-Rashid, S. E. Clapham, A. Hadzovic, J. N. Harvey, A. J. Lough, R. H. Morris, *J. Am. Chem. Soc.* **2002**, *124*, 15104-15118.

[33] B. Askevold, M. M. Khusniyarov, W. Kroener, K. Gieb, P. Müller, E. Herdtweck, F. W. Heinemann, M. Diefenbach, M. C. Holthausen, V. Vieru, L. F. Chibotaru, S. Schneider, *Chem. Eur. J.* **2015**, *21*, 579-589.

[34] A formally 14-electron pyramidal Ru(II) complex (Cy-PSiP)RuO^{t}Bu has also been reported: MacInnis, M. C.; McDonald, R.; Ferguson, M. J.; Tobisch, S.; Turculet, L. *J. Am. Chem. Soc.* **2011**, *133*, 13622−13633

[35] J. C. Babón, M. A. Esteruelas, A. M. López, *Chem. Soc. Rev.* **2022**, *51*, 9717-9758.

[36] D. E. Prokopchuk, A. Collado, A. J. Lough, R. H. Morris, *Dalton Trans.* **2013**, *42*, 10214-10220.

[37] M. J. Burn, M. G. Fickes, J. F. Hartwig, F. J. Hollander, R. G. Bergman, *J. Am. Chem. Soc.* **1993**, *115*, 5875-5876.

[38] S. W. Kohl, L. Weiner, L. Schwartsburd, L. Konstantinovski, L. J. W. Shimon, Y. Ben-David, M. A. Iron, D. Milstein, *Science* **2009**, *324*, 74-77.

[39] A TBP stucture for **A** also supports the P,P–*cis* to *trans* isomerization observed.

[40] A. M. R. Hall, P. Dong, A. Codina, J. P. Lowe, U. Hintermair, *ACS Catal.* **2019**, *9*, 2079-2090.

[41] A. Friedrich, M. Drees, S. Schneider, *Chem. Eur. J.* **2009**, *15*, 10339-10342.

[42] In an attempt to access directly a hydride-containing active species, a solution of complex **2** was exposed to H_2 (4 bar) prior to use in catalysis. A very broad signal was observed at ~$\delta(^1H)$ –9 consistent with a *trans* dihydride complex. This complex decomposed on removal of solvent. As the hydride chemical shift is likely to be infuenced by dihydrogen bonding from $H_3B{\cdot}NMeH_2$ under operando conditions, that will also be concentration-dependent (see ref. 17,36), we are relucant to over interpret these observations. Importantly, no signifciant change in inital rate or the induction period relative to pre-catalyst **2** was observed when this solution was used in catalysis.

[43] A. Antiñolo, M. A. Esteruelas, C. García-Yebra, J. Martín, E. Oñate, A. Ramos, *Organometallics* **2019**, *38*, 310-318.

[44] G. Guella, C. Zanchetta, B. Patton, A. Miotello, *J. Phys. Chem. B.* **2006**, *110*, 17024-17033.

[45] Under conditions of no H_2O, polymer is selectivey formed with very high molecular weight (M_n = 250,000 g/mol, $Đ$ = 1.8). While the mechansim of chain-growth termination is yet to be fully resolved, this observation provides further control over the final polymer. With 500 ppm water the isolated polymer is much shorter (M_n = 54,000 g/mol, $Đ$ = 1.6). While cannot discount that the borates observed come from chain degradation with water, the narrow dispersity suggests that if this is occuring it is rather selective.

[46] Running the reaction with no special precuation for ingress of air resulted in no-catalytic turnover.

[47] C. Alamillo-Ferrer, G. Hutchinson, J. Burés, *Nature Rev. Chem.* **2023**, *7*, 26-34.

[48] There is no measurable induction period at 0.33 mol% loading, but H_2 evolution is so fast (~ 10 s) that meaningful kinetics could not be collected.

[49] J. A. Widegren, R. G. Finke, *J. Mol. Cat. A* **2003**, *198*, 317-341.

[50] D. Evans, J. A. Osborn, G. Wilkinson, *J. Chem. Soc. A* **1968**, 3133-3142.

[51] D. E. Ryan, K. A. Andrea, J. J. Race, T. M. Boyd, G. C. Lloyd-Jones, A. S. Weller, *ACS Catal.* **2020**, *10*, 7443-7448.

[52] M. Bochmann, *Organometallics* **2010**, *29*, 4711-4740.

Entry for the Table of Contents

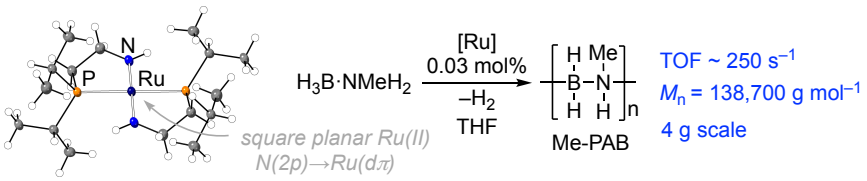

Square planar, Ru(II), Ru(^{i}Pr$_2$PCH$_2$CH$_2$NH)$_2$ is the first formed species on simple dehydrohalogenation of RuCl$_2$(^{i}Pr$_2$PCH$_2$CH$_2$NH$_2$)$_2$ using ^{t}BuOK, a pre-catalyst system that promotes very fast and selective amine-borane dehydropolymerization to form high molecular weight polyaminoborane.